UCLA
UCLA Previously Published Works

Title
A Method to Measure the Rate of Glaucomatous Visual Field Change

Permalink
https://escholarship.org/uc/item/3kj8r52b

Journal
Translational Vision Science & Technology, 7(6)

ISSN
2164-2591

Authors
Caprioli, Joseph
Mohamed, Lilian
Morales, Esteban
et al.

Publication Date
2018-11-30

DOI
10.1167/tvst.7.6.14

Peer reviewed

eScholarship.org Powered by the California Digital Library
University of California

tvst

https://doi.org/10.1167/tvst.7.6.14

Article

A Method to Measure the Rate of Glaucomatous Visual Field Change

Joseph Caprioli[1], Lilian Mohamed[1,2], Esteban Morales[1], Alessandro Rabiolo[1,3], Nathaniel Sears[1], Hirunpatravong Pradtana[1], Reza Alizadeh[1], Fei Yu[1,4], Abdelmonem A. Afifi[4], Anne L. Coleman[1], and Kouros Nouri-Mahdavi[1]

[1] Jules Stein Eye Institute, David Geffen School of Medicine, University of California Los Angeles, Los Angeles, CA, USA
[2] Department of Ophthalmology, Cairo University Faculty of Medicine, Cairo, Egypt
[3] Department of Ophthalmology, University Vita-Salute, IRCCS San Raffaele, Milan, Italy
[4] Department of Biostatistics, Fielding School of Public Health, University of California Los Angeles, Los Angeles, CA, USA

Correspondence: Joseph Caprioli, Glaucoma Division, Jules Stein Eye Institute, 100 Stein Plaza, Los Angeles, CA 90095, USA. e-mail: caprioli@jsei.ucla.edu

Received: 13 June 2018
Accepted: 16 September 2018
Published: 30 November 2018

Keywords: Glaucoma Rate Index; pointwise exponential progression; glaucomatous perimetric progression; visual field

Citation: Caprioli J, Mohamed L, Morales E, Rabiolo A, Sears N, Pradtana H, Alizadeh R, Yu F, Afifi AA, Coleman AL, Nouri-Mahdavi, K. A method to measure the rate of glaucomatous visual field change. Trans Vis Sci Tech. 2018;7(6):14, https://doi.org/10.1167/tvst.7.6.14
Copyright 2018 The Authors

Purpose: To develop a method to measure the rate of glaucomatous visual field (VF) deterioration and to identify fast progressors.

Methods: Retrospective, longitudinal, observational study of 8486 eyes of 4610 glaucomatous patients with ≥6 VFs and ≥3 years of follow-up. A Glaucoma Rate Index (GRI) was calculated. VF locations were partitioned into exponential decay or exponential improvement models. A pointwise rate of change (PRC) was estimated with an exponential fit and expressed as the percent/year change of the age- and location-matched normal perimetric range, presented as a spatially conserved VF map. PRCs were summed and normalized with boundary rates set by simulated decaying and improving VF series on a scale of −100 to +100, respectively.

Results: A total of 89,704 VF examinations with 425,039 test location series was used. Median follow-up and number of VFs/eye were 9.7 years and 9 VFs, respectively. Initial and final mean deviations (±SD) were −4.2 (±5.2) and −5.7 (±6.4) dB. The proportions of test locations designated as decayed, improved, and unchanged were 13%, 4%, and 83%, respectively. Mean PRCs for decay, improvement, and no change were −3.7 (±4.7)%/y, 2.5 (±2.6)%/y, and −0.5 (±2.1)%/y, respectively. The number of eyes with negative and positive GRIs was 5802 (68%) and 2390 eyes (28%), respectively. The proportion of eyes defined as fast progressors was 6.8%.

Conclusions: GRI provides a robust measure of glaucomatous VF change, operates without discontinuity over the entire perimetric range, and can be used to identify fast progressors.

Translational Relevance: This study describes a novel method that can help the clinician to determine VF progression.

Introduction

The anticipation of disease progression is the foundation of glaucoma management. An important aspect of evaluation is the acquisition of serial automated perimetric measurements to characterize a patient's past visual field (VF) changes and to extrapolate the findings as a probability for ongoing VF deterioration. If this is performed adequately, timely intervention to slow or stop additional worsening may be appropriately applied.[1]

Statistical models of perimetric change have been developed to support the clinical evaluation of serial VFs. Methods vary, with the broadest categories being either trend-based or event-based. Generally, trend-based algorithms are useful for generating a rate of VF change that may be used to estimate the probability of future deterioration. Pointwise linear regression (PLR) is a widely used trend analysis that regresses the sensitivities at each test location over time.[2] Critics argue that the linear core of the regression may not be best suited for biological

This work is licensed under a Creative Commons Attribution-NonCommercial-NoDerivatives 4.0 International License.

systems; linear models assume a constant additive rate of VF deterioration, but as the VF deteriorates, the relative changes that can occur become more clinically significant and are restricted by a measurement floor (0 decibels [dB]).[3] An alternative trend-based approach uses an exponential regression to better model glaucomatous VF measurements.[4–6] Although global trend analysis can be used to determine the overall rate of change in VF series, it does not model regional deterioration, which is common in early to moderate glaucoma.[3,7] Existing indices are designed to measure abnormalities, not rates of change. It has been repeatedly shown that the global index mean deviation (MD) is nonspecific for glaucoma and insensitive to localized VF changes, and pattern standard deviation (PSD) decreases as damage advances in moderate to advanced disease.[8] Visual field index (VFI) has its own problems with discontinuity at more advanced stages of loss.[9] VFI can also miss early diffuse VF damage due to a ceiling effect.[9] Event-based analyses are binary algorithms that depend on defined criteria for progression and alert the user when these criteria are met. Guided progression analysis (GPA) of the Humphrey Field Analyzer (Carl Zeiss Meditec, Inc., Dublin, CA) is the most widely used event-based analysis; this proprietary tool identifies significant pointwise progression based on statistical probabilities estimated from at least three sequential VFs. Although it has been shown to be slightly more sensitive than PLR or the use of Advanced Glaucoma Intervention Study (AGIS) scores, it lacks information on rates and therefore is not easily used to predict future change.[10] Regardless of which model is used, the algorithm should take into account the appropriate age- and location-matched normal values and aging rates of change.[11,12]

There is no consensus about which statistical model is most appropriate for clinical or investigative use. Efforts to measure and define VF change remain hampered by several inconvenient realities of VF progression.[1] Glaucomatous VF deterioration is neither linear nor constant over time, and psychophysical measurements are notoriously noisy. These inherent properties can limit the detection of VF progression. Different regions of the same VF can show fast worsening, slow worsening, no change, or even improvement.[5] One can certainly measure the rate of change of these indices, but the usefulness of these estimated rates are hindered by their demonstrated limitations.

We present a method for calculating the Glaucoma Rate Index (GRI) with serial glaucomatous VFs, which provides a standardized estimate of the rate of VF change. We apply this approach in a large database of serial glaucomatous VFs. GRI offers a conceptually simple, rapid, and real-time approach to estimate the rate of VF change. It is accompanied by a spatially conserved VF map that indicates the status of each test location, whether worsening, improving, or without change. The GRI can also be used to identify fast progressors: those patients whose glaucoma is worsening at a high rate and who require appropriately aggressive therapeutic intervention.

Patients and Methods

The database used to develop and test GRI was compiled from a collection of consecutive VF data of patients with glaucoma who were treated at the Glaucoma Division of the Stein Eye Institute, University of California, Los Angeles (UCLA). This study was approved by the UCLA Human Research Protection Program, was performed in accordance with the tenets set forth in the Declaration of Helsinki, and complied with Health Insurance Portability and Accountability Act regulations. All VF examinations were performed with a Humphrey Field Analyzer with 24-2 or 30-2 test patterns, with a size III white stimulus, and with either full threshold or the Swedish Interactive Thresholding Algorithm (SITA) standard testing strategies. All VFs in a series from a particular eye were either all full threshold or all SITA standard; serial VFs obtained with different testing algorithms were not mixed. The database used included a large cohort of glaucoma patients who were treated by the Glaucoma Division of the Stein Eye Institute, with a minimum follow-up period of 3 years and a minimum of six VF tests. Since data were retrospectively collected, patients were tested at different intervals according to the indications provided by the glaucoma specialist caring for them. Since the purpose of the study was to present a universal method to measure rates of glaucoma progression, we did not exclude patients based on type of glaucoma, visual acuity, age, changes in medical therapy, or execution of laser or surgical intervention. All VFs that were satisfactorily completed as judged by a perimetrist were included; no other reliability criteria were imposed. VF locations were excluded from the analysis if they were part of the physiologic blind spot or if any two of the initial three measurements at a test location had threshold sensitivities of 0 dB. All statistical analyses were

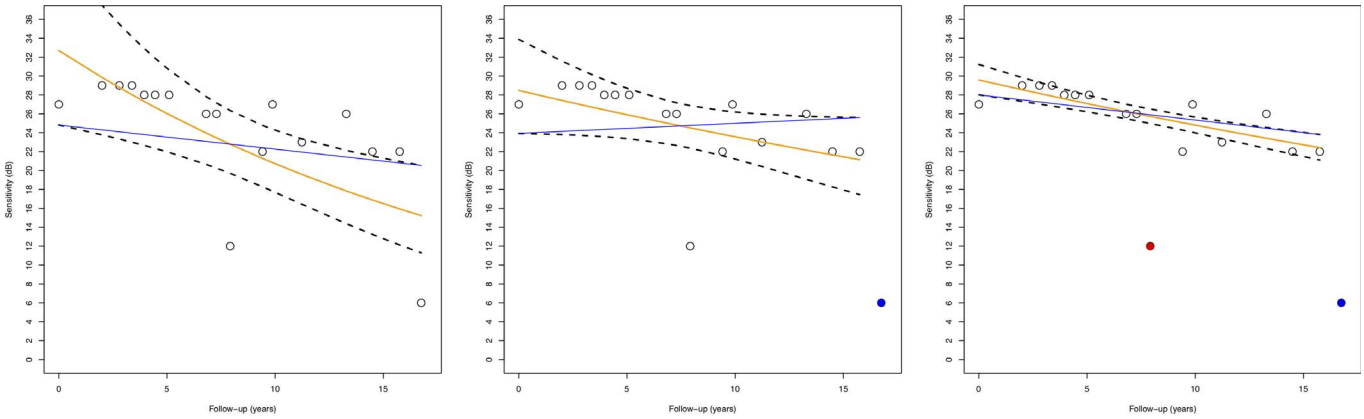

Figure 1. The application of two noise filters to remove outliers. (*Left*) Raw data are shown. (*Middle*) Cook's distance correction is applied, which tends to remove outliers at the ends of the data series, which unduly affect the slope (*blue dot*). (*Right*) The method of Studentized residuals was next applied, which tends to remove outliers away from the ends of data series (*red dot*). In this example, the sequential application of these two filters results in the criteria for decay being met at this test location.

performed with the open-source programming language R.[13]

The process of generating a GRI score for each eye is described as follows:

1. An a priori screening was used to categorize each pointwise series as either decaying or improving, according to whether its linear trend was negative or positive, respectively.
2. Pointwise exponential regression (PER) of each series was performed. For VF locations with a negative trend, the decay PER model was applied, expressed as $y = e^{(a+bx)}$, where y = sensitivity in decibels, a = constant, b = regression coefficient (slope), and x = time in years. This model had an asymptote as a floor (0 dB). The estimates of a and b were obtained by regressing $\ln(y)$ on x. For VF points with a positive trend, we used a mirror image approach, where the exponential function had an asymptote as a ceiling (the normal age-matched value for that particular test location plus twice its standard deviation). The function of the improvement model is expressed as $Y - y = e^{(a+bx)}$, where y = sensitivity (decibels) at time x (years), Y = the normal age-matched threshold sensitivity + 2 SD, a = constant, and b = regression coefficient (slope).
3. Outliers were removed on the basis of their Cook's distance[14] and the Studentized residual test[15] (Fig. 1). All threshold values in a pointwise series for a test location were sequentially removed with Cook's distance >1 and a |Studentized residual| >3. The former method removes influential points at the extremities able to leverage the regression slope, while the latter method removes points with high root mean squared error away from the ends of the series, which can affect the y-intercept and the width of the confidence interval (CI). According to Weisberg,[16] these cutoffs are recommended to balance removing too many versus too few influential points.
4. The pointwise rate of change (PRC) of each series, expressed as a percentage of the entire normal perimetric range, corrected for age and location, was calculated.[11,12] PRC was calculated as the change between the initial ($y(0)$) and final ($y(t)$) values of the PER model fit divided by the age- and location-matched dynamic range of threshold sensitivity (in dB) for each test location in the VF. Thus, the rates of change are expressed as the proportion (%) change per year of the entire perimetric range, corrected for location and age. Locations that met the criteria for change and had a positive PRC were marked as improving. Locations that met the criteria for change and had a negative PRC were marked as decaying. Decaying PRC locations were further divided into slow and fast decay based on the distribution of PRC values: the test locations in the fastest (most negative) quartile of decaying locations were categorized as "fast decay." The PRCs are displayed graphically to show the spatial relationships of the pointwise rates of change (Fig. 2) and are used to calculate the GRI for each eye.

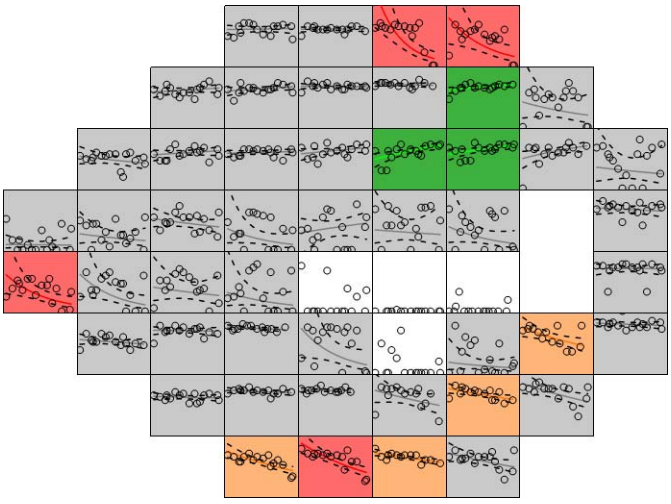

Figure 2. Graphical representation of regional VF changes. The series of sensitivity measurements over time are shown for each test location. Test locations with immeasurable rates are shown as *white boxes*. *Gray boxes* indicate that those locations do not meet criteria for change. *Orange* indicates slow decay, *red* indicates fast decay, and *green* indicates improvement.

5. The 90% CI of the exponential regression line was used to determine whether a VF location was categorized as no change, decay, or improvement. If the rate defined by the slope of the line joining the points from initial bottom to final top of the CI bands (Fig. 3) is negative and the rate exceeded the 95th percentile of the normal aging rate, then the rate was counted as significant and was used to define the decay rate at that location. In the case of an improving PER, if the rate defined by the line joining the points from initial top of the CI band to final bottom of the CI band was positive, then the rate was counted as significant and was used to define the improving rate at that location (Fig. 3). This approach required the points to be within a sufficiently tight fit and to have a sufficiently negative or positive trend in order to be considered either decaying or improving. Test locations that did not meet either of these criteria were designated as "no change." These are presented as a spatially conserved VF map, which indicates the status of each test location, whether worsening, improving, or without change, as shown in Figure 2.
6. A GRI score for each eye was calculated by summing the PRCs for all test locations that met the above criteria for change. If none of the 54 test locations analyzed in a VF series had significant change, then this eye was assigned a GRI value of "0." GRI scores were normalized from −100 to +100, where −100 represents an extreme rate of decay and +100 represents an extreme rate of improvement. To construct the

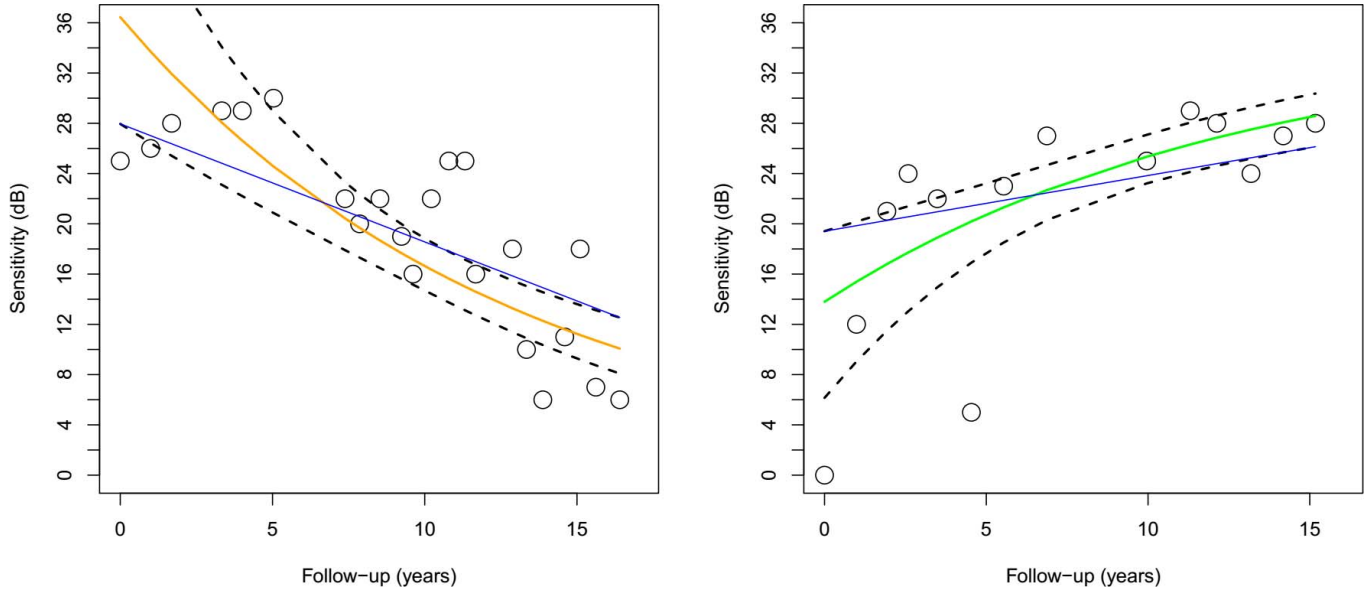

Figure 3. (*Left*) Decay PER of VF series with 90% CI (*dotted line*). The minimum rate (index rate) was defined by the slope of linear regression (*blue line*) joining the points from the initial bottom to the final top of the CI, the index slope. (*Right*) Improvement PER of VF series with 90% CI (*dotted line*). The minimum rate was defined by the slope of the linear regression (*blue line*) joining the points from the initial top to the final bottom. If the index rates met additional criteria for change (see text), then the median rates (*orange* and *green lines* in the examples above) were used as the measured rates for that location.

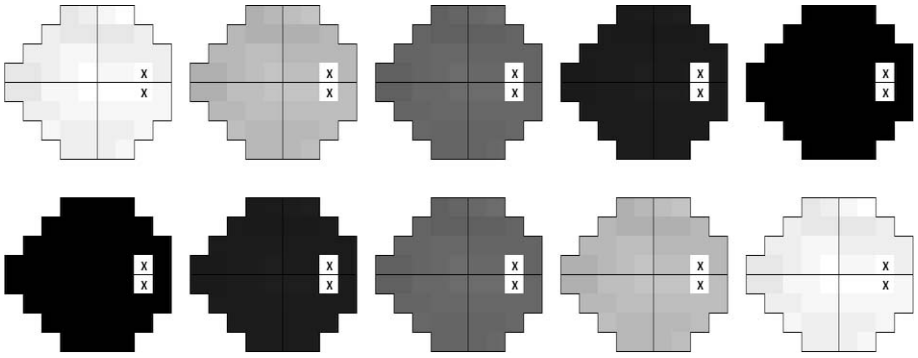

Figure 4. (*Top*) The extreme decay model, which shows perimetric decay from age-matched normal values to perimetric blindness (0 dB) in 20 years. This extreme model was assigned a Glaucoma Change Index score of −100. (*Bottom*) Extreme improvement model, which shows perimetric improvement from 0 dB to age-matched normal values in 20 years. This extreme model was assigned a Glaucoma Change Index of +100.

extreme decay model, we started with location-matched normal eyes at 60 years of age. Over a span of 20 years, each starting decibel value was decreased at a constant (linear) rate so that the final decibel value would be 0. The PER model was then fit to this series, and the PRCs were summed. This value was used for the decay normalization and was set to −100. The inverse was performed for improvement, and the sum of the PRCs was normalized to +100 (Fig. 4). Eyes within the fastest decaying decile of GRI values were designated as fast progressors.

To facilitate a comparison of GRI with other indices, we estimated a cutoff value for GRI for changing and stable VF series. For each eye, bootstrapping, a well-known statistical technique to account for variance, was performed.[17] Briefly, we randomly selected n VF exams, where n is the total number of examinations for the eye with replacement (a VF may appear multiple times in the same sample). A new GRI was calculated based on the randomly selected n exams and subtracted from the original GRI of the eye. This was performed 1000 times, and a 90% CI of GRI for each eye was calculated. Decaying eyes (GRI < 0) were grouped by GRI values to the nearest integer. Within each group, we calculated the percentage of eyes that had a 90% CI upper limit < 0. The GRI value of the group having 50% of eyes meeting this criterion was set as the decaying cutoff. To better estimate the GRI at the 50% cutoff, the locally weighted scatterplot smoothing (LOWESS) fit was applied to the scatterplot.[18] The same process also was employed for GRI > 0 to estimate a cutoff for improvement.

The stability of GRI with regard to the number of points used in its calculation was evaluated by measuring the effect of changing the number of VF visits for each eye in the calculated GRIs through sequentially removing each of the data points one at a time and recalculating a new GRI for each instance. The difference between each of the recalculated GRIs from the original GRI was calculated. The mean GRI differences for each eye was plotted against the number of VFs in each eye to show the magnitude of GRI variability as a function of the number of VF visits.

Results

Dataset

A total of 8486 eyes of 4610 patients were included, with a mean (±SD) baseline age of 64.6 (±13.9) years (Table 1). There were 4239 (49.9%) right eyes and 4247 (50.1%) left eyes. There was a total of 89,704 VF

Table 1. Demographic Data for the VF Database

Total No. of Patients	4,610
Total no. of eyes	8,486
Right eyes	4,239 (49.9%)
Left eyes	4,247 (50.1%)
Mean baseline age, y	64.6 (±13.9)
Mean initial MD, dB	−4.2 (±5.2)
Mean final MD, dB	−5.7 (±6.4)
Median no. VFs	9
Median follow-up, y	9.5
Total no. of VF exams	89,704
SITA standard	80,503 (90%)
Full threshold	9,201 (10%)

Table 2. Number of Test Locations and Mean (±SD) PRC for the Overall, No Change, Decay, Slow Decay, Fast Decay, and Improvement Categories

	Overall	No Change	Decay	Slow Decay	Fast Decay	Improvement
Number of locations	425,026 (100%)	352,985 (83%)	55,102 (13%)	42,904 (10%)	12,198 (3%)	16,939 (4%)
PRC mean (±SD)	−0.8%/y (±3.0)	−0.5%/y (±2.1)	−3.7%/y (±4.7)	−2.1%/y (±1.1)	−9.0%/y (±4.0)	2.5%/y (±2.6)

examinations, of which 80,503 (90%) were SITA standard and 9201 (10%) were full threshold exams. Median follow-up was 9.5 years, with a median number of nine VFs. The median time (interquartile range [IQR]) between two consecutive examinations was 8.9 (7.1) months. The initial MD was −4.2 (±5.2) dB, and the final MD was −5.7 (±6.4) dB. There was a total of 425,039 test location series. Mean (±SD) false negative responses, false-positive responses, and fixation losses per eye were 4.8% (±4.7%), 4.8% (±4.9%), and 0.2% (±0.2%), respectively.

Application of the Cook's distance criterion removed 118,251 (2.8%) points from the raw data. Application of the Studentized residual criterion removed an additional 13,691 (0.3%) points from the raw data. The number of measurements removed from a single test location for a single VF series ranged from 0 to 3. The maximum number of measurements removed from all test locations for a single VF series was 92. The mean ± SD number of measurements removed from a single examination was 1.5 ± 4.9 (range 0–54). Exclusion of ≥26 measurements (more than half of the VF test locations) from a single VF occurred in 1.1% of all examinations. A total of 16,246 (3.2%) locations were excluded from the analysis because they had threshold sensitivity values of 0 dB in two out of the first three tests. The median (IQR, range) number of locations removed from a single eye was 0 (0, 0–44). Exclusion of >26 locations from a single eye occurred in 69 (0.8%) eyes.

Pointwise Rates of Change

The percentage of test locations that showed decay was 13%; 10% were categorized as slow decay and 3% as fast decay. Fast decay was defined by the fastest quartile of all decaying rates, which corresponds to a PRC of less than –5%/y. Improvement was measured at 4% of the test locations, while 83% displayed no change (Table 2). The mean PRC for all locations was −0.8 (±3.0)%/y; −3.7 (±4.7)%/y for decaying locations, 2.5 (±2.6)%/y for improving locations, and −0.5 (±2.1)%/y for locations designated as no change (Fig. 5). Pointwise change is graphically represented with color-coded VF maps, which display all serial sensitivities for each test location over time (Fig. 2).

Glaucoma Rate Index

The number of eyes with negative GRI values (worsening) was 5802 (68.4%), and the number of eyes with positive values (improving) was 2390 (28.2%). A total of 294 (3.5%) eyes were assigned a GRI value of 0. Progressors were further partitioned into slow and fast categories: the cutoff for fast progressors, arbitrarily set as the fastest decay decile of GRI values, corresponds to a GRI less than −37. The same process applied to MD rate generated a value of −0.97 dB/y. The total number of fast progressors was 575 eyes (6.8%), as shown in Figure 6.

GRI Stability

The mean GRI difference calculated for stability was 0.3 (±2.2) for the entire group. The range of variability became narrower as the number of observations increased in a VF series (Fig. 7). This SD is about 2% to 10% of the entire GRI scale when eight or more VFs are used.

Bootstrap and the Relationship of MD Versus GRI

A scatterplot of the percentage of eyes per GRI bin that had a 90% CI below 0 and the LOWESS fit applied to the scatterplot is shown in Figure 8. Based on the LOWESS fit, a GRI cutoff of approximately −6 includes 50% of eyes with a GRI 90% CI < 0. As the GRI decreases, the percentage of eyes with GRI 90% CI < 0 increases (Fig. 8). A scatterplot of MD rate versus GRI is shown in Figure 9.

Discussion

We propose a novel method to measure VF rate change that includes a rate index, which we call the GRI. The technique is based on exponential fits of

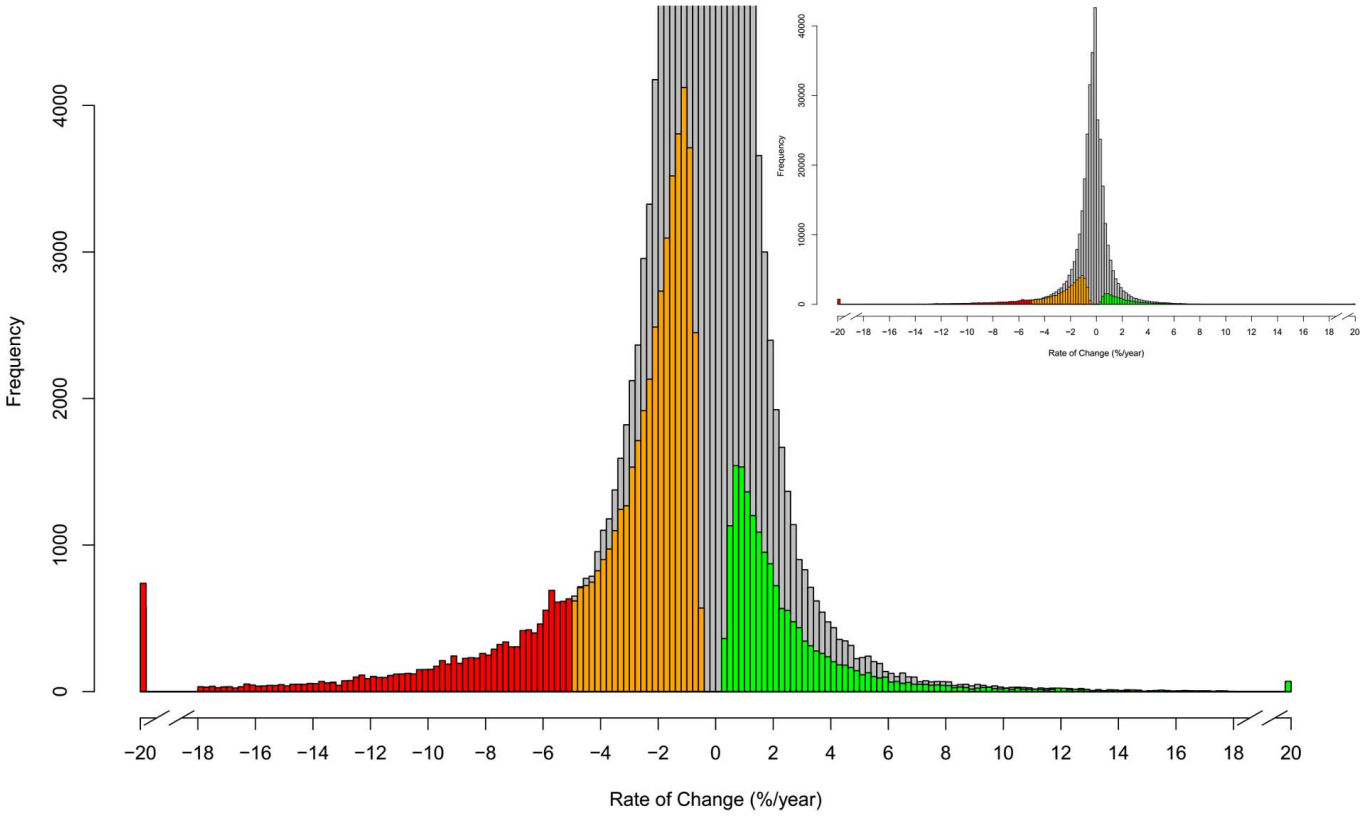

Figure 5. The frequency distribution of PRC for all test locations expressed as percentage rate of change per year. *Gray* indicates test locations assigned to the category of no change, with a mean value −0.5%/y. *Orange* indicates test locations designated as slower decay with a mean value of −2.1%/y. *Red* indicates test locations designated as fast decay with cutoff at −5%/y and a mean value of −9.4%/y. *Green* indicates improvement with a mean value of +2.5%/y.

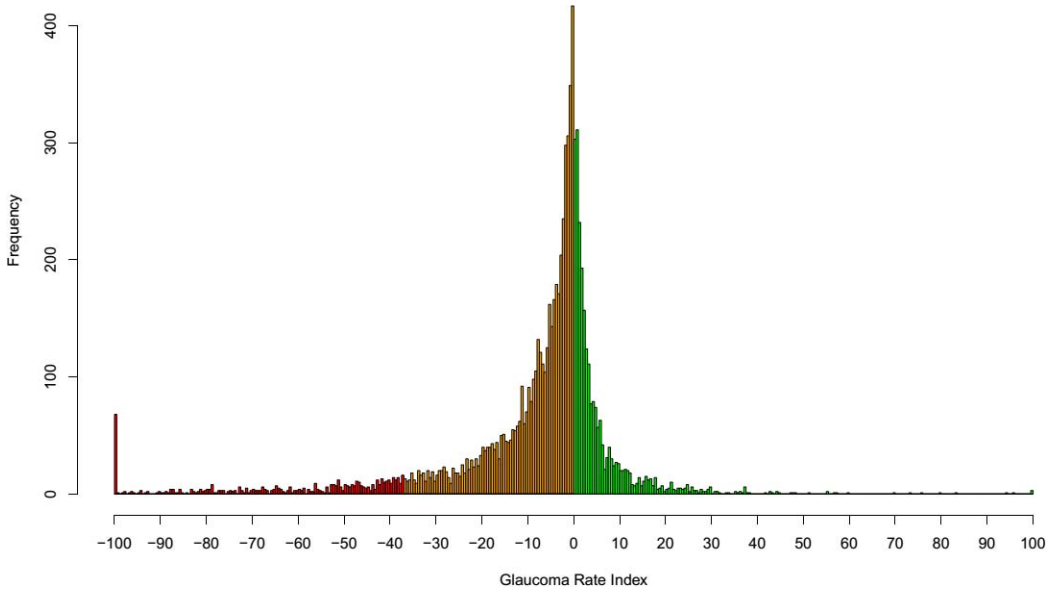

Figure 6. The frequency distribution of the GRI for all eyes. The cutoff for fast progressors is arbitrarily set as the lowest decile of all the worsening eyes (GRI < 0), which is GRI ≤ -37. Indices of eyes represented in *orange* (62% of all eyes) are more slowly progressive, *red* indicates fast progressors (6.8%), and those represented in *green* show improvement (28%); 3% have a GRI value of 0.

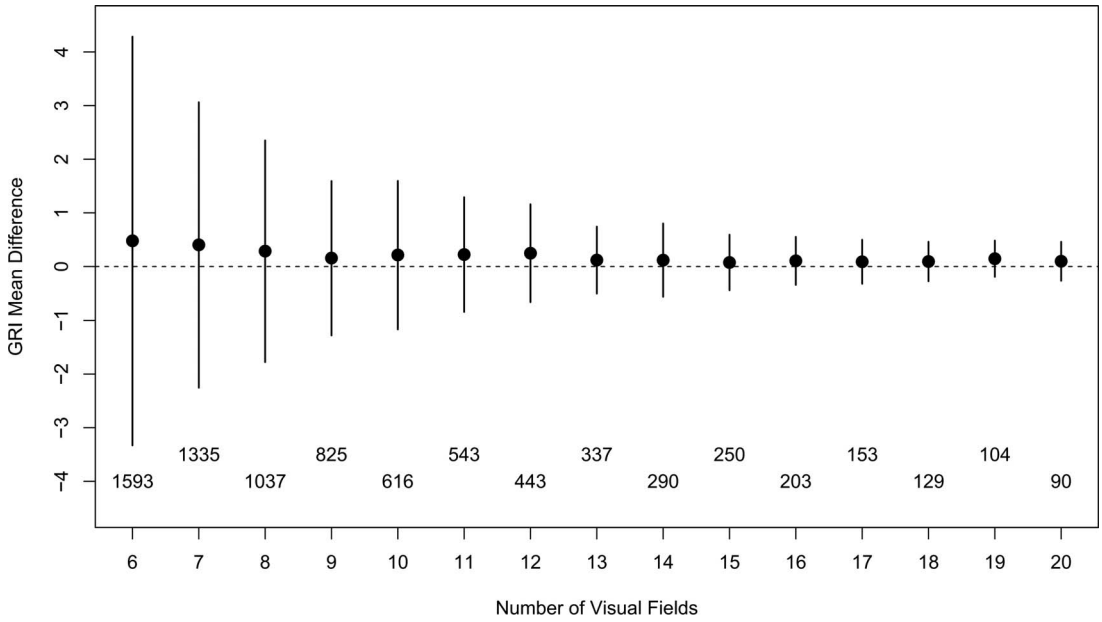

Figure 7. Plot representing the mean (± SD) GRI difference for eyes as a function of number of VF visits. By comparing these results to the mean (± SD) of the entire group, it shows that the range of variability increases with fewer VF visits (six VFs) as compared to a narrow range of variability with more VF visits (greater than eight VFs). The SD of GRI has a magnitude of ≤2 when eight or more VFs are used.

pointwise threshold sensitivities of serial VF tests. This index might be considered analogous to the VFI, but it is actually an index for rate of change rather than for stage of disease. The method also provides a graphical presentation of spatially conserved, pointwise rates, in which the change in status of each test location is shown. The GRI estimates the rate of change on a normalized scale and can be used to categorize worsening eyes into fast progressors and slow progressors (Fig. 10).

GRI is based on PER (rather than linear regression). Previous papers have described the use of PER to model VF change. Chen et al.[6] compared the behavior of linear, exponential, and logistic models in serial VF examinations and found that although logistic models fit glaucomatous VF behavior well over a long period of time, an exponential model provided the best overall predictions. Azarbod et al.[4] showed that exponential models are effective across a wide range of severities and can predict future change better than can linear models. Exponential approaches appear to be better than either linear or other nonlinear models in patients with moderate to severe glaucomatous damage because values typically approach 0 dB in an asymptotic fashion, a property that cannot be accounted for with linear techniques without discontinuities.[6,19,20] Although it is based on PERs, GRI uses a linear trend as a first step to categorize each location as improving or decaying. The nonlinear exponential regression model exists in two different, but symmetrical and specular forms: decaying and improving (Fig. 3). The a priori categorization with a linear trend is required to select the appropriate model for a given VF series.

Another feature of the approach reported here is that it preserves spatial information. The regression of global indices (e.g., MD, VFI) are insensitive to focal glaucomatous progression and can be more affected by those conditions, causing a generalized reduction of threshold sensitivities, such as cataract progression.[21] Conversely, pointwise approaches can retain their perimetric spatial relationships and allow the measurement of the rate of progression at every test location. Katz and colleagues[22] compared regression of global indices, clusters of locations, and single locations to identify perimetric progression. In their study, regression of global indices failed to recognize localized damage with a rate of <1 dB/y and an annual frequency of VF testing. On the other hand, global indices are generally more specific than pointwise approaches, since they require a higher magnitude of change to detect progression.[22,23] The GRI includes only those test locations with significant change, as it is defined by the method. Other indices, including permutation analyses of pointwise linear regression (PoPLR) and GPA, also consider only locations significantly deteriorating. Global rates of VF progression, conversely, take into consideration

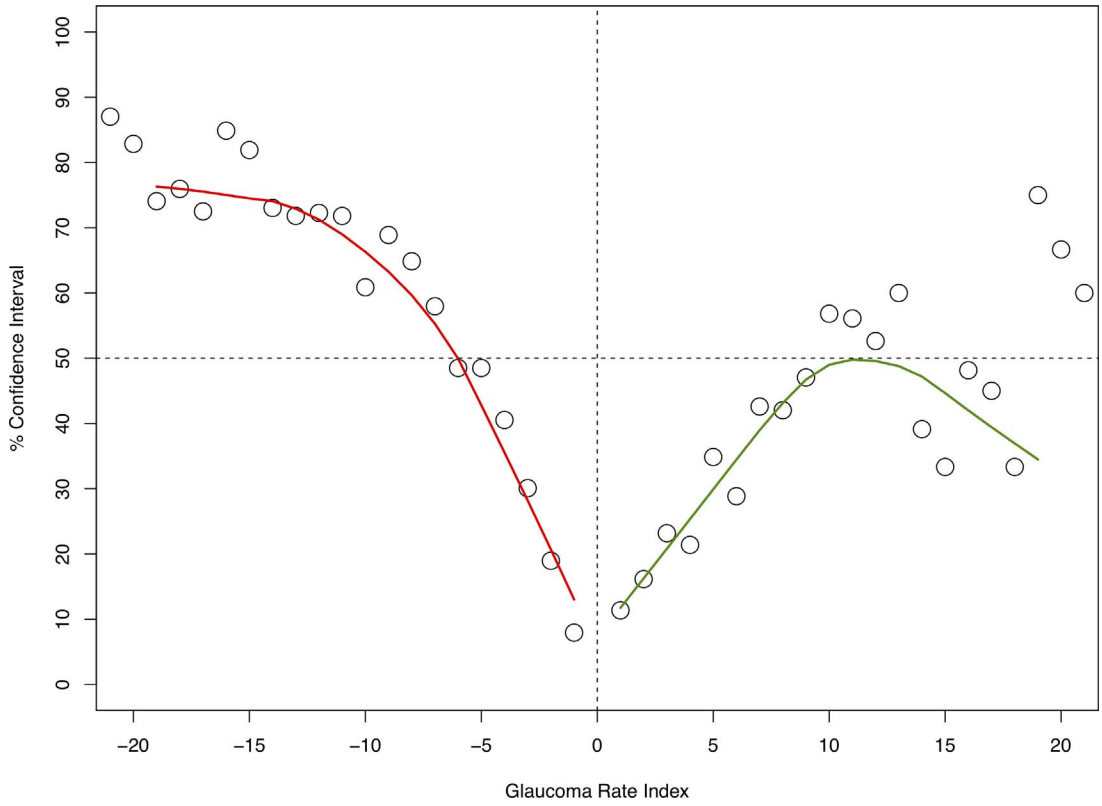

Figure 8. Plot of the percentage of decaying (*red line*) and improving (*green line*) eyes with a GRI 90% CI upper limit <0 and lower limit >0 with the locally weighted scatterplot smoothing (LOWESS) fit applied, respectively. For each eye, *n* random VF examinations were selected, where *n* is the total number of examinations. A new GRI was calculated and subtracted from the original GRI. This was performed 1000 times, and a 90% CI of the GRI was calculated. Decaying eyes (GRI < 0) and improving eyes (GRI > 0) were binned by integral GRI values, and the percentage of eyes within each bin that had a GRI 90% CI upper limit of <0 and lower limit of >0 was calculated, respectively. The bin with 50% of eyes (*dotted line*) that met this criterion was selected as the cutoff value for decaying and improving GRI, respectively.

all test locations, including those points that are stable throughout the VF series and points with absolute defects at baseline. Inclusion of these data, however, has the potential to obscure the signal of clinically important localized changes.

GRI is presented as a clinical tool to alert the physician about patients at risk for visual disability. The standardization to a scale of −100 to +100 facilitates intuitive interpretation and also allows for improvement.[5] The method presented here allows the user to choose any number or any group of consecutive VFs for analysis, so long as there are at least six. For example, one may choose to analyze the VFs only after a major change in treatment and compare this with the GRI before the change if a sufficient number of VFs are available. A caveat is that the fewer number of VFs included in a series, the more the potential error in its estimation. This variability is reasonable with eight or more VF tests (1 SD is approximately 2%–10% of the range of GRI); thus for best results, eight or more VF tests should be used to improve the accuracy of the index. Although it can always be mathematically calculated, we recommend GRI calculation based on an adequate number of test locations. We suggest a minimum of 26 locations, which corresponds to half of the VF test locations. This requirement might not be satisfied in case of far-advanced glaucoma, where multiple locations can be entirely excluded in case of a threshold sensitivity value of 0 dB in two out of the first three tests. This was, however, an uncommon event in this very large database of all comers and occurred only in 0.8% of all eyes.

The authors have found that the clinical application of this technique to be very helpful and has allowed us to identify progression more often than when using a qualitative evaluation of VF series or GPA printouts, and it has allowed us to make this judgment much more rapidly. The index is normalized and does not behave discontinuously in advanced

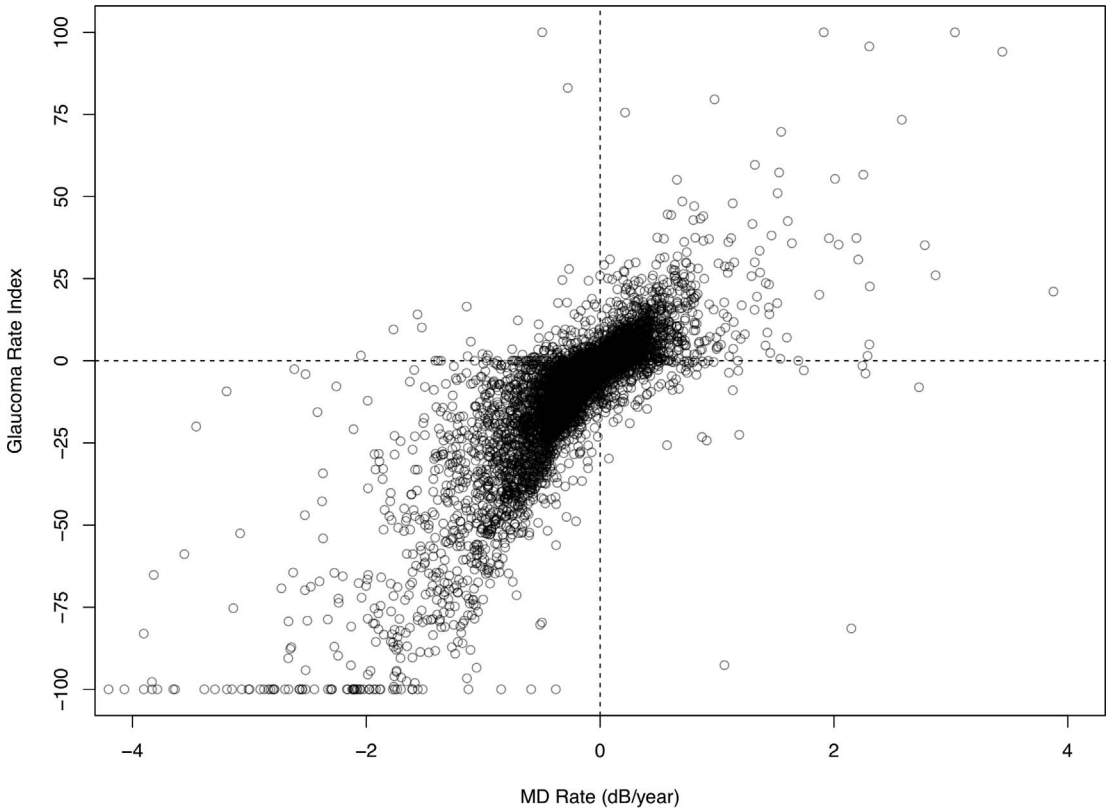

Figure 9. A scatterplot of the GRI versus MD rate.

disease like PSD or VFI; in advanced disease, PSD actually decreases and VFI becomes quite variable.[24]

In addition to the numerical generation of GRI, all test locations are displayed in a spatially conserved, color-coded VF map (Fig. 2), which allows the clinician to visualize the degree and pattern of VF changes in a rapid, user-friendly manner. This approach is not unique to the GRI. For instance, the Progressor software (OBF Labs UK Ltd, Wiltshire, UK), which is based on PLR, also provides a similar graphical output.[25] In the graphical presentation of GRI, color codes are based on the PRC values. Specifically, we require serial sensitivity measurements for each test location to be within a sufficiently tight fit and to have a sufficiently negative or positive trend to be categorized as decaying or improving. Those test locations not meeting either of these criteria were designated as "no change." Test locations decaying at a rate faster than 5%/y were categorized as fast decay. Thus, all test locations were categorized as either (1) unmeasurable, (2) fast decay, (3) slow decay, (4) no change, or (5) improving.

We also derived a cutoff for GRI to distinguish slowly progressing eyes from more rapidly progressing eyes. While not all eyes that demonstrate visual loss need aggressive treatment (or in some cases any treatment), a certain proportion of the fastest progressing eyes deserve that consideration. Chauhan et al.[26] measured rates of glaucoma progression in a large clinical population under routine clinical care and found that 5.8% of patients were fast progressors. In another study by Baril et al.[27] the proportion of fast progressing eyes was 3.9% and 9.4% for eyes receiving medical and surgical glaucoma treatments, respectively. Prevalence of fast progressors, however, may vary across different populations since it is dependent on many factors, such as age, stage of disease, treatment, and subtype of glaucoma.[28] In addition, the way to define and measure fast progression remains arbitrary. Most of the previous studies defined fast progression as the rate of MD decline, usually ranging from −1 dB/y to −2 dB/y. As discussed earlier, however, MD rate is based on the entire VF, and it could underestimate profound but localized changes, delaying the recognition of fast progressors at risk. VFI rate is similar in this regard and may additionally suffer from a ceiling effect and discontinuity in severe stages.[29] Event-based approaches do not provide rates of progression. Methods based on PLR could be employed; however,

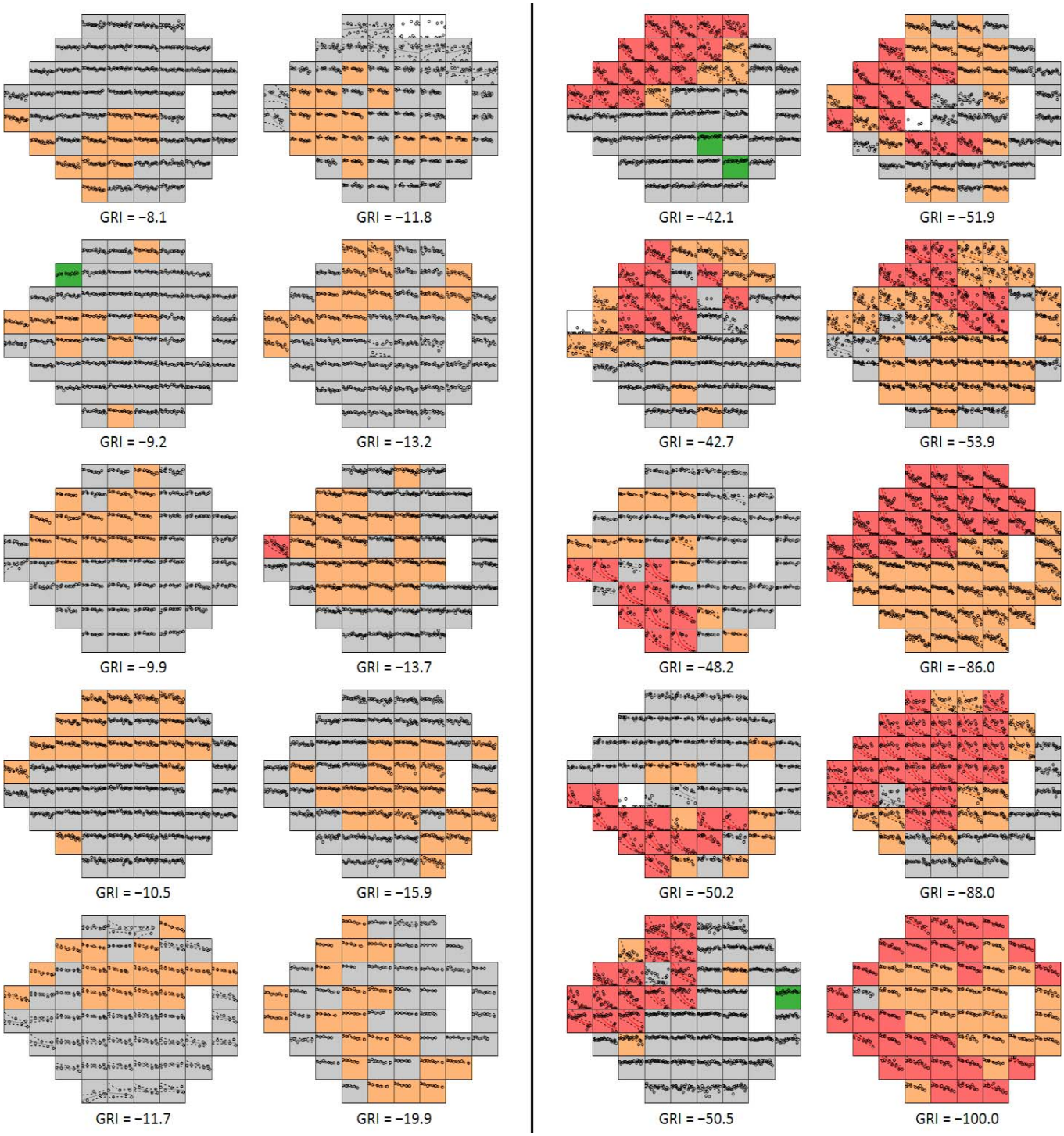

Figure 10. GRI estimates the rate of change on a normalized scale and can be used to categorize worsening eyes into "fast progressors" (GRI < -37, examples in right two columns) and slower progressors ($-6 <$ GRI > -37, examples in left two columns).

they have not been investigated for this purpose, and it is unclear which criteria should be used to identify fast progressing eyes. Medeiros and colleagues[30] proposed a model to evaluate rates of progression with an empirical Bayes estimate of rates of change and clustered VF progression into four groups, based on similarities of their trajectories. The authors claimed that their method was better than simple linear regression, especially in identifying fast progressors. In this study, we propose a method for identifying fast

progressors. Based on the results of previous studies regarding the prevalence of fast progressors, we defined the fastest decile of negative GRI values as those belonging to fast progressors.[26–28,30] The fastest decile of negative MD rate corresponded to a value of −0.97 dB/y, which resembles the cutoff of −1 dB/y adopted by other studies.[26,27] The GRI value for fast progressors is largely arbitrary and is presented as an example of how this identification might be accomplished. Where one draws the cutoff ultimately depends on many factors, including patient-related factors (other risk factors, longevity, patients' desires, etc.), public health concerns, and resource availability.

Recently published findings reported that VF data can undergo both short- and long-term improvement after medical or surgical intervention.[5,31–34] We have included the possibility of improvement in our method by applying an exponential fit to VF test locations with an a priori improving trend. An inverted exponential decay fit with a ceiling asymptote of the age-matched normal +2 SD value was applied, as opposed to applying a constant multiplicative (linear) rate of improvement to a longitudinal VF series, which seems to not be physiologically appropriate.[5] In addition, other trend-based and event-based methods (except for the current version of GPA) could be used to detect improvement.

VF examination is a subjective test and is characterized by intrinsic variability. Presence and stage of glaucoma are well-known contributing factors.[35] Uncorrected refractive error, patient motivation and instruction, fatigue, technician experience, time of day, season, race, cognitive level, and percentage of false-positive responses have been recognized as additional sources of variability.[36–40] Large fluctuations are an obstacle to the proper modeling of VF data, and several strategies have been employed to reduce the noise.[41] A first measure relies on controlling known causes, such as repetition of examinations scored as poorly reliable and training and motivation of both patient and technical staff. Trend-based methods based on regression of global indices (i.e., MD, VFI) are less influenced by pointwise variability since they are averaged measures. Bryan et al.[41] proposed a model called global visit effects, which takes into account known and unknown factors affecting all the locations of the same examination. When applied to longitudinal data, correction of global visit effects improved the estimation of true rates of progression and increased the ability to predict future changes. Interestingly, the global visit effects model performed better than the simple correction for established factors of variability, suggesting a contribution by other, unknown variables.

We used Cook's distance and Studentized residuals to remove outliers that may unduly influence the model fit and to improve the signal-to-noise ratio. The former method tends to remove influential outliers at the extremities of the data series, which can dramatically change the slope of the regression line. The latter method tends to exclude outliers away from the ends of the series with high root mean square error, which can affect the y-intercept and the width of the CI. About 3% of all measurements were removed with this approach. A previous study showed a difference in results obtained before and after Cook's correction.[5] In the current study, exclusion of $\geq$26 points (more than half of VF test locations) from a single examination occurred in only 1.1% of all examinations, suggesting that outlier removal performed by GRI can omit a large portion or even an entire examination. This can mitigate the effect of the aforementioned factors, inducing variability at every test location at the same visit, and could represent an alternative to other proposed methods, such as proposed by the global visit model.[41] Our data indicate, however, that removal of a large part of an examination is an uncommon event, and the majority of visits (74.8%) had no points excluded at all.

As for other algorithms, GRI carries some assumptions. Table 3 summarizes the assumptions made by GRI and other algorithms. All methods, including GRI, assume that VF progression is caused by glaucoma; this reduces the specificity of all techniques and remains a clinical issue for the examiner to differentiate. Although test locations are spatially correlated and glaucoma damage usually conforms to the anatomy of the retinal nerve fiber layer, GRI treats all points equally.[42] This represents an assumption that is not unique to GRI (it is also found with GPA, algorithms based on PLR, and PoPLR).[2,43,44] Data derived from pointwise linear or exponential regressions can be postprocessed with spatial filters, and this can improve the prediction ability of both models.[7] Spatial correlation among test locations is taken into account by very few algorithms, such as ANSWERS, recently proposed by Zhu and colleagues.[45] Although such an index seems to perform better than MD regression and PoPLR, further testing is required for validation. GRI is based on PER, and therefore it assumes that VF decay follows an exponential model over time. As linear

Table 3. List of Assumptions Made by Some Algorithms to Assess Glaucomatous VF Progression

Assumption	Algorithms
Perimetric changes are related to glaucoma	All
VF decay follows an exponential model over time	GRI
VF decay follows a linear model over time	Simple PLR, PoPLR
VF sequence is not right-censored (data can be extrapolated forward below 0 dB)	Simple PLR
VF sequence is not left-censored (data can be extrapolated infinitely backward)	Simple PLR, GRI
Rate of change of nonprogressing eyes is null	PoPLR
Eyes can either progress or remain stable, and no difference exists among eyes in the same category	Event-based methods (e.g., GPA, AGIS, CIGTS)
Locations with 0 dB at baseline are perimetrically blind	GRI, GPA
Eyes with severe VF damage do not progress further	All
VF does not improve	GPA

CIGTS, Collaborative Initial Glaucoma Treatment Study.

regression is vulnerable to both left and right censoring effects, exponential regression is vulnerable to left censoring effects since the backward extrapolation of a series could lead to unfeasibly high or low sensitivities in the case of decay or growth exponential models, respectively. In this regard, GRI assumes that there is a time at which a discontinuity in the series occurred and glaucomatous VF damage "began" for an eye. Backward extrapolation, however, is not clinically relevant, whereas forward extrapolation is useful for prediction. GRI treats locations with a threshold sensitivity of 0 dB in any two of the initial three examinations as locations of perimetric blindness, and progression or improvement cannot be established at such locations. This assumption is not unique to GRI since other approaches (e.g., GPA) omit locations with low sensitivities at baseline.

The limitations of this study should be reviewed. There is no gold standard by which the specificity and sensitivity of GRI can be objectively evaluated; there is an inherent deficiency of external validation to evaluate perimetric progression, given the changing relationship between structural and functional correlates as a function of the severity of disease.[46] Computer-simulated VF sequences with predetermined rates and patterns of progression may help in this regard. GRI may miss early diffuse loss from glaucoma, since GRI includes only test locations that meet criteria for change. While early glaucoma may cause a mild generalized reduction of whole-field sensitivity, such changes are not common or specific for glaucoma. Application of the method requires extra time and resources to export data and apply external calculations and display. This could be remedied easily by incorporation of the algorithm into standard VF software. The cutoff for fast progressors was set arbitrarily. This could be modified, depending on the goals of recognizing and treating such patients in the particular population being treated and the treatment resources available to that population. The utility of GRI in clinical research regarding progression and treatment effects would need further study. Studies are underway to test this method in a separate database and to evaluate its predictive results compared to those of other established indices.

In summary, we present a GRI to summarily estimate visual change rates in patients with glaucoma. It is expected to be more sensitive to localized glaucomatous damage compared to global indices, and it is able to model improvement, which has recently been shown to be a potentially important clinical scenario in glaucoma after significant reduction of the intraocular pressure. The GRI operates across a wide range of VF severities. Use of the accompanying presentation of spatially preserved pointwise rates improves the utility of the technique for individual patients.[5] We believe that these properties are complementary and that their presence in a single model would be useful for clinicians and investigators. Finally, GRI has the ability to flag eyes as fast progressors and can be used to help guide the appropriate use of resources to improve the outcomes of patients at high risk for visual disability.

Acknowledgments

Supported by an unrestricted grant from Research to Prevent Blindness, the National Institutes of Health Grant 5K23EY022659 (KN-M), and the Simms/Mann Family Foundation.

Disclosure: **J. Caprioli**, None; **L. Mohamed**, None; **E. Morales**, None; **A. Rabiolo**, None; **N. Sears**, None; **H. Pradtana**, None; **R. Alizadeh**, None; **F. Yu**; None; **A.A. Afifi**, None; **A.L. Coleman**, None; **K. Nouri-Mahdavi**, None

References

1. Caprioli J. The importance of rates in glaucoma. *Am J Ophthalmol*. 2008;145:191–192.
2. Viswanathan AC, Fitzke FW, Hitchings RA. Early detection of visual field progression in glaucoma: a comparison of PROGRESSOR and STATPAC 2. *Br J Ophthalmol*. 1997;81:1037–1042.
3. Otarola F, Chen A, Morales E, Yu F, Afifi A, Caprioli J. Course of glaucomatous visual field loss across the entire perimetric range. *JAMA Ophthalmol*. 2016;134:496–502.
4. Azarbod P, Mock D, Bitrian E, et al. Validation of point-wise exponential regression to measure the decay rates of glaucomatous visual fields. *Invest Ophthalmol Vis Sci*. 2012;53:5403–5409.
5. Caprioli J, de Leon JM, Azarbod P, et al. Trabeculectomy can improve long-term visual function in glaucoma. *Ophthalmology*. 2016;123:117–128.
6. Chen A, Nouri-Mahdavi K, Otarola FJ, Yu F, Afifi AA, Caprioli J. Models of glaucomatous visual field loss. *Invest Ophthalmol Vis Sci*. 2014;55:7881–7887.
7. Morales E, de Leon JM, Abdollahi N, Yu F, Nouri-Mahdavi K, Caprioli J. Enhancement of visual field predictions with pointwise exponential regression (PER) and pointwise linear regression (PLR). *Trans Vis Sci Technol*. 2016;5:12.
8. Bengtsson B, Heijl A. A visual field index for calculation of glaucoma rate of progression. *Am J Ophthalmol*. 2008;145:343–353.
9. Artes PH, O'Leary N, Hutchison DM, et al. Properties of the statpac visual field index. *Invest Ophthalmol Vis Sci*. 2011;52:4030–4038.
10. Nouri-Mahdavi K, Hoffman D, Ralli M, Caprioli J. Comparison of methods to predict visual field progression in glaucoma. *Arch Ophthalmol*. 2007;125:1176–1181.
11. Heijl A, Lindgren G, Olsson J. Normal variability of static perimetric threshold values across the central visual field. *Arch Ophthalmol*. 1987;105:1544–1549.
12. Spry PG, Johnson CA. Senescent changes of the normal visual field: an age-old problem. *Optom Vis Sci*. 2001;78:436–441.
13. R Development Core Team. *R: A Language and Enviroment for Statistical Computing*. Vienna, Austria: R Foundation for Statistical Computing; 2010.
14. Cook RD. Detection of influential observation in linear regression. *Technometrics*. 1977;19:15–18.
15. Afifi A, May S, Clark VA. *Practical Multivariate Analysis*. 5th ed. Boca Raton, FL: Chapman and Hall/CRC; 2011:100–102.
16. Weisberg S. *Applied Linear Regression*. 3rd ed. Hoboken, NJ: John Wiley and Sons, Inc. 2005:194–210.
17. Efron B, Tibshirani RJ. *An Introduction to the Bootstrap*. New York City, NY: Chapman & Hall; 1993:1–430.
18. Cleveland WS. *Visualizing Data*. Summit, NJ: Hobart Press; 1993:1–340.
19. Caprioli J, Mock D, Bitrian E, et al. A method to measure and predict rates of regional visual field decay in glaucoma. *Invest Ophthalmol Vis Sci*. 2011;52:4765–4773.
20. Pathak M, Demirel S, Gardiner SK. Nonlinear, multilevel mixed-effects approach for modeling longitudinal standard automated perimetry data in glaucoma. *Invest Ophthalmol Vis Sci*. 2013;54:5505–5513.
21. Chauhan BC, Drance SM, Douglas GR. The use of visual field indices in detecting changes in the visual field in glaucoma. *Invest Ophthalmol Vis Sci*. 1990;31:512–520.
22. Katz J, Gilbert D, Quigley HA, Sommer A. Estimating progression of visual field loss in glaucoma. *Ophthalmology*. 1997;104:1017–1025.
23. Smith SD, Katz J, Quigley HA. Analysis of progressive change in automated visual fields in glaucoma. *Invest Ophthalmol Vis Sci*. 1996;37:1419–1428.
24. Lee JM, Cirineo N, Ramanathan M, et al. Performance of the visual field index in glaucoma patients with moderately advanced visual field loss. *Am J Ophthalmol*. 2014;157:39–43.
25. Fitzke FW, Hitchings RA, Poinoosawmy D, McNaught AI, Crabb DP. Analysis of visual field progression in glaucoma. *Br J Ophthalmol*. 1996;80:40–48.

26. Chauhan BC, Malik R, Shuba LM, Rafuse PE, Nicolela MT, Artes PH. Rates of glaucomatous visual field change in a large clinical population. *Invest Ophthalmol Vis Sci*. 2014;55:4135–4143.
27. Baril C, Vianna JR, Shuba LM, Rafuse PE, Chauhan BC, Nicolela MT. Rates of glaucomatous visual field change after trabeculectomy. *Br J Ophthalmol*. 2017;101:874–878.
28. Heijl A, Bengtsson B, Hyman L, Leske MC, Early Manifest Glaucoma Trial G. Natural history of open-angle glaucoma. *Ophthalmology*. 2009;116:2271–2276.
29. Rao HL, Senthil S, Choudhari NS, Mandal AK, Garudadri CS. Behavior of visual field index in advanced glaucoma. *Invest Ophthalmol Vis Sci*. 2013;54:307–312.
30. Medeiros FA, Zangwill LM, Weinreb RN. Improved prediction of rates of visual field loss in glaucoma using empirical Bayes estimates of slopes of change. *J Glaucoma*. 2012;21:147–154.
31. Cohen SL, Rosen AI, Tan X, Kingdom FAA. Improvement of the visual field index in clinical glaucoma care. *Can J Ophthalmol*. 2016;51:445–451.
32. Musch DC, Gillespie BW, Palmberg PF, Spaeth G, Niziol LM, Lichter PR. Visual field improvement in the collaborative initial glaucoma treatment study. *Am J Ophthalmol*. 2014;158:96–104, e102.
33. Ventura LM, Porciatti V. Restoration of retinal ganglion cell function in early glaucoma after intraocular pressure reduction: a pilot study. *Ophthalmology*. 2005;112:20–27.
34. Wright TM, Goharian I, Gardiner SK, Sehi M, Greenfield DS. Short-term enhancement of visual field sensitivity in glaucomatous eyes following surgical intraocular pressure reduction. *Am J Ophthalmol*. 2015;159:378–385, e371.
35. Blumenthal EZ, Sample PA, Berry CC, et al. Evaluating several sources of variability for standard and SWAP visual fields in glaucoma patients, suspects, and normals. *Ophthalmology*. 2003;110:1895–1902.
36. Junoy Montolio FG, Wesselink C, Gordijn M, Jansonius NM. Factors that influence standard automated perimetry test results in glaucoma: test reliability, technician experience, time of day, and season. *Invest Ophthalmol Vis Sci*. 2012;53:7010–7017.
37. Mutlukan E. The effect of refractive blur on the detection sensitivity to light offsets in the central visual field. *Acta Ophthalmol (Copenh)*. 1994;72:189–194.
38. Kutzko KE, Brito CF, Wall M. Effect of instructions on conventional automated perimetry. *Invest Ophthalmol Vis Sci*. 2000;41:2006–2013.
39. Gracitelli CPB, Zangwill LM, Diniz-Filho A, et al. Detection of glaucoma progression in individuals of African descent compared with those of European descent. *JAMA Ophthalmol*. 2018;136:329–335.
40. Diniz-Filho A, Delano-Wood L, Daga FB, Cronemberger S, Medeiros FA. Association between neurocognitive decline and visual field variability in glaucoma. *JAMA Ophthalmol*. 2017;135:734–739.
41. Bryan SR, Eilers PH, Lesaffre EM, Lemij HG, Vermeer KA. Global visit effects in point-wise longitudinal modeling of glaucomatous visual fields. *Invest Ophthalmol Vis Sci*. 2015;56:4283–4289.
42. Pascual JP, Schiefer U, Paetzold J, et al. Spatial characteristics of visual field progression determined by Monte Carlo simulation: diagnostic innovations in glaucoma study. *Invest Ophthalmol Vis Sci*. 2007;48:1642–1650.
43. O'Leary N, Chauhan BC, Artes PH. Visual field progression in glaucoma: estimating the overall significance of deterioration with permutation analyses of pointwise linear regression (PoPLR). *Invest Ophthalmol Vis Sci*. 2012;53:6776–6784.
44. Nassiri N, Moghimi S, Coleman AL, Law SK, Caprioli J, Nouri-Mahdavi K. Global and pointwise rates of decay in glaucoma eyes deteriorating according to pointwise event analysis. *Invest Ophthalmol Vis Sci*. 2013;54:1208–1213.
45. Zhu H, Crabb DP, Ho T, Garway-Heath DF. More accurate modeling of visual field progression in glaucoma: ANSWERS. *Invest Ophthalmol Vis Sci*. 2015;56:6077–6083.
46. Lee JW, Kim EA, Otarola F, et al. The fast component of visual field decay rate correlates with disc rim area change throughout the entire range of glaucomatous damage. *Invest Ophthalmol Vis Sci*. 2015;56:5997–6006.